Radiation Cross Calibration Based on GF-1 Side Swing Angle

Yong Xie[1], Zui Tao[2, *], Wen Shao[3], John J. Qu[4], Hai Huan[3] and Chuanyang Tian[3]

Abstract: Radiation cross-calibration is an effective method to check and verify the accuracy and stability of sensor measurements. Satellites with high radiation accuracy are used to calibrate satellites with low radiation accuracy. In order to ensure the reliability of the radiation cross-calibration method, we propose to obtain the gain and offset of the GaoFen-1 satellite by linear regression after the radiation cross-calibration of the satellite with low precision and compare with the official coefficient. Finally, we get the relationship between the error in radiation cross-calibration results and side swing angle. The linear correction coefficients of each band are: 0.618, 0.625, 0.512 and 0.474. The results show that after the method is corrected by the linear correction coefficient, the error caused by the side swing angle during the cross-calibration of the orbital radiation is reduced. The accuracy of radiation cross-calibration is improved, the frequency of calibration is improved and the requirements of remote sensing applications in the new era are adapted.

Keywords: Side swing angle, GF-1, radiation cross calibration, correction.

1 Introduction

GaoFen-1 (GF-1) was successfully launched on April 26, 2013. It is equipped with a 2-meter resolution full-color/8-meter resolution multi-spectral camera and a 16-meter resolution multi-spectral wide-format camera. The GF-1 imaging ground width can reach more than 60 km and the wide-spectrum multi-spectral camera can reach more than 800 km [Bai (2013)]. The altitude of the satellite orbit is 645 km, the viewing range of the high-resolution camera side is 25 km and the Wide-spectrum camera coverage period is 4 days when the side-swing function is not used. The panchromatic and multi-spectral (PMS) camera coverage period is 41 days [Bai (2013); Han and Xie (2016)].

At present, the on-orbit radiation calibration of satellite sensors commonly used at home and abroad mainly includes three methods: site calibration, star calibration and cross-calibration [Wei, Zhang, Zhang et al. (2018)]. The cost required for star calibration and

---

[1] School of Geography and Science, Nanjing University of Information Science and Technology, Nanjing, 210044, China.

[2] Institute of Remote Sensing and Digital Earth, Chinese Academy of Sciences, Beijing, 100089, China.

[3] School of Electronic & Information Engineering, Nanjing University of Information Science and Technology, Nanjing, 210044, China.

[4] Environmental Science and Technology Center, George Mason University, 4400 University Drive, Fairfax, VA, 22030, U.S.A

* Corresponding Author: Zui Tao. Email: taozui@radi.ac.cn.

site radiometric calibration is more expensive than radiation cross-calibration. At this stage, the GF-1 satellite only conducts site radiation calibration once a year. Less radiation calibration frequency and errors generated during the calibration process result in lower accuracy of the GF-1 radiation cross-calibration and poor radiation stability.

In this paper, the multi-band remote sensor the MODIS with high accuracy of radiometric calibration is selected as the reference radiation reference for the visible light band. The radiation cross-calibration of GF-1 is carried out, which reduces the error of calibration results and improves the calibration frequency and accuracy.

2 Cross-radiation calibration method

Cross-radiation calibration is a kind of radiometric calibration. Firstly, we select satellite images with the same observations of two satellites [Lin, Liu, Xiao et al. (2018)]. Then we perform spectral matching and spatial matching on it and establish the relationship between the reference sensor's radiance and the target sensor, and use the calibration coefficient of the reference remote sensor to achieve the target remote sensing calibration (the main process is shown in Fig. 1 below).
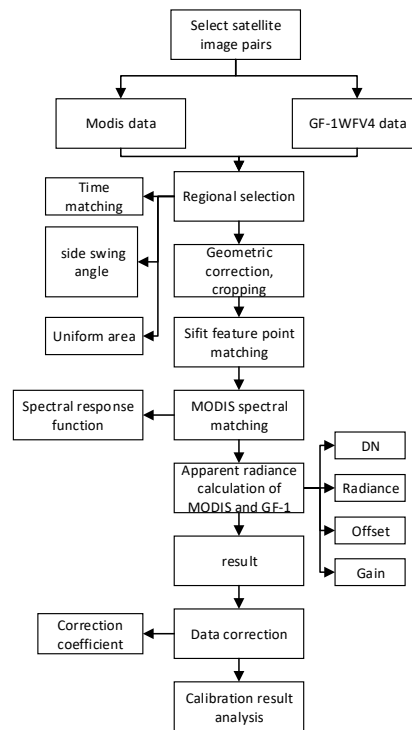

Figure 1: Cross-radiation calibration process

The apparent radiance of the cross-calibration of the MODIS and GF-1/WFV4 radiation is calculated by the Eq. (1):

$$L_{M/GF-1}^{i} = m^{i} \times (DN_{M/GF-1}^{i} - n_{set}^{i}) \tag{1}$$

$L^i_{M/GF-1}$ *is* the apparent radiance of the *i-th* band of the MODIS and GF-1; m^i is the gain factor of the *i-th* band of the MODIS and GF-1; n^i_{set} is the offset of the *i-th* band of the MODIS and GF-1; $DN\ ^i_{M/GF-1}$ is the digital count (DN) value of the *i-th* band of the MODIS and GF-1 [Duan, Song, Qin et al. (2018)].

Then according to the digital count value of the four bands for GF-1, the linear fitting is performed to obtain the fitting coefficient. The formula is expressed in Eq. (2):

$$L^i_M = a^j \times DN^j_{GF-1} + b^j \tag{2}$$

a^j is the gain factor of the *j-th* band of the MODIS and GF-1, b^j is the offset of the *j-th* band of the MODIS and GF-1, DN^j_{GF-1} is the digital count value of the four bands of GF-1. L^i_M is the apparent radiance of the *j-th* band of the MODIS [Yao, He, Zhang et al. (2017)].

3 Data processing and analysis

3.1 Research area

In this paper, we choose Dunhuang as a radiation correction field (40.04 °N ~ 40.28 °N, 94.17 °E ~ 94.05 °E). The Dunhuang radiation correction field has the advantages of flat terrain, uniform surface and good directional characteristics. It is suitable for visible light near-infrared remote sensors to perform absolute radiation calibration in orbit [Han and Xie (2016)].

3.2 Reference satellite selection

MODIS sensor is mainly mounted on the Terra and Aqua stars. It has 36 discrete spectral bands and a wide spectral range. The resolution of the GF-1 wide-format camera is 16 m and the resolution of the MODIS is 250 m, 500 m, 1000 m (the GF-1 and MODIS load performance tables are shown in Tab. 1). Since the resolution of bands 1 and 2 of the MODIS is 250 m, this paper selects the MODIS satellite image with a resolution of 500 m as the reference sensor and conducts radiation cross-calibration on the GF-1 [Gao, Gu, Tao et al. (2016)].

Table 1: Introduction of GF-1, MODIS, satellite bands and performance

		GF-1		MODIS	
		Band	**Spectral**	**Band**	**Spectral**
	R	3	0.63-0.69	1	0.62-0.67
Multispectral	**G**	2	0.52-0.59	4	0.545-0.565
	B	1	0.45-0.52	3	0.459-0.479
	NIR	4	0.77-0.89	2	0.841-0.876
Resolution		16 m		250 m, 500 m, 1000 m	
Side swing ability		35°		55°	
Revisiting time		4 days		Almost a day	

3.3 Calculation of spectral matching factors

The effective image pairs of the MODIS and GF-1/WFV4 include: (1) when the satellite transits, the required time interval is less than 2 hours and there is no cloud above the radiation correction field; (2) the selected area is in the central area of the scene [Qin, Suzanne, Sun et al. (2018)].

4 Data analysis

4.1 Comparison of single side and side view

Fig. 2 is a cross-calibration result of the GF-1/WFV4 and MOIS images with a side swing angle and Fig. 3 is a cross-calibration result of the GF-1/WFV4 and MOIS images with a no side swing angle. The X-axis is the DN value of GF-1/WFV4 and the Y-axis is the apparent radiance of the MODIS. Gain and error are shown in Tab. 2. The error without side swing angle is 3.04%, 5.26%, 5.33% and 5.10%. Red visible light band error is the largest, reaching 5.33%. The accuracy of the cross calibration is verified to meet the quantitative requirements. The errors of the side pendulum are 5.07%, 7.60%, 6.67% and 5.73%. Through two sets of effective scenes, in the case of side swing angles and no side swing angles, their accuracy of correlation coefficients and offsets have a certain impact. When the satellite performs on-orbit radiation cross-calibration, the side swing angles have an effect on the accuracy of their radiation cross-calibration.
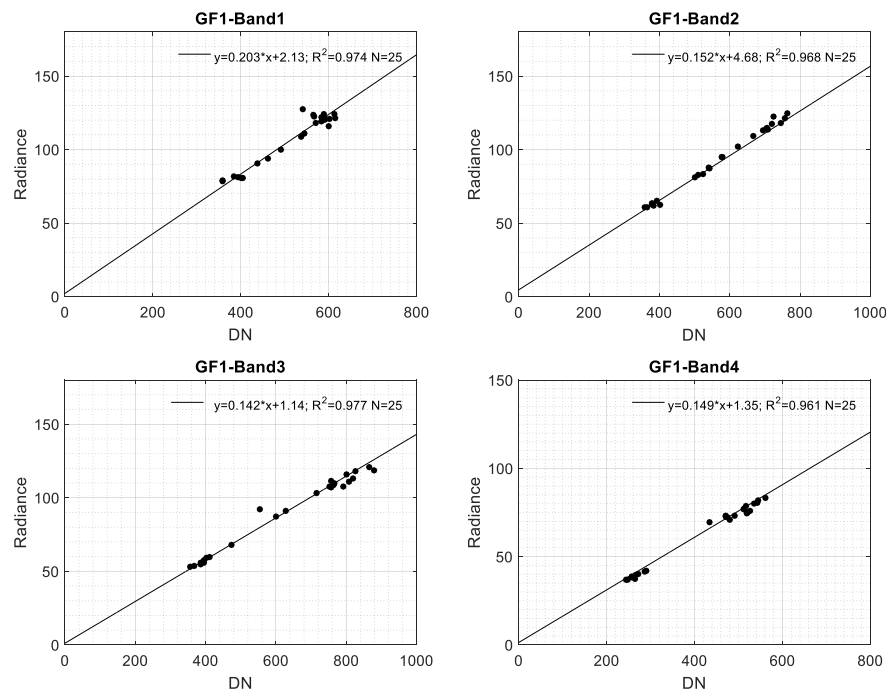

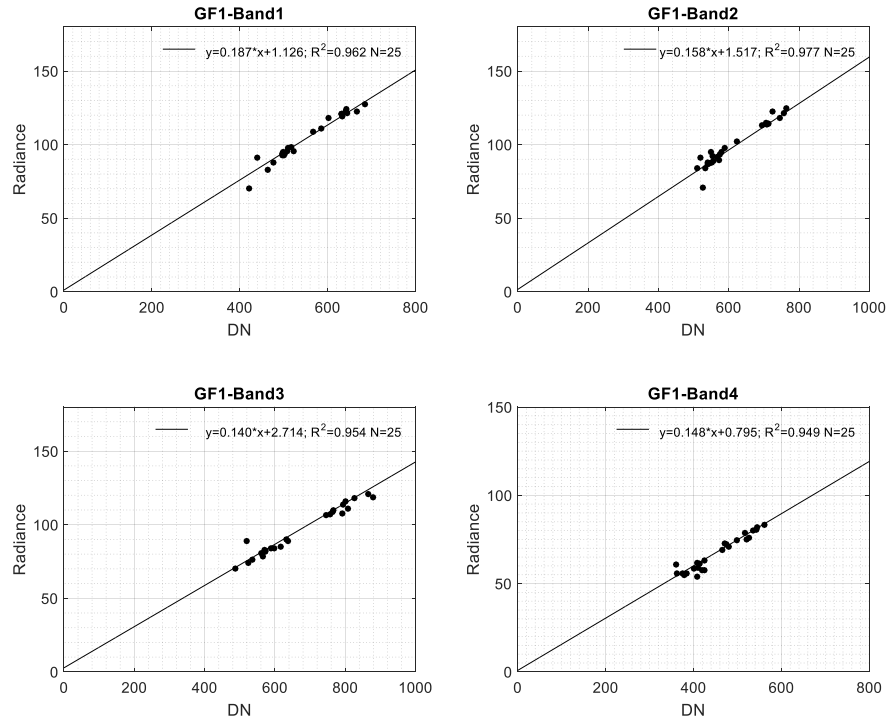**Figure 2:** Cross-calibration results of GF-1/WFV 4 and MODIS

Figure 3: Cross-calibration results of GF-1/WFV 4 and MODIS

Table 2: Comparison of gain error between side swing angle and official calibration coefficient

GF-1/WFV4	Official	None-angle		Angle	
		Gain	*Error（%）*	*Gain*	*Error（%）*
Band1	0.197	0.203	3.04	0.187	-5.07
Band2	0.171	0.162	-5.26	0.158	-7.60
Band3	0.150	0.142	-5.33	0.140	-6.67
Band4	0.157	0.149	-5.10	0.148	-5.73

4.2 Effective image error results of 19 sets of side swing angles for 2013-2018

In this paper, the effective images of the 19 sets of the side swing angles in the Dunhuang area from 2013 to 2018 and the corresponding two sets of the stars below the star point are selected, as shown in Fig. 4. The X-axis is the side swing angle and the Y-axis is the error of the radiation cross-calibration. The official calibration results are: 0.618, 0.625, 0.512 and 0.474. It indicates that the side swing angle is linear with the result of the cross calibration. The error of the GF-1 cross-calibration result increases with the increase of the side swing angle.
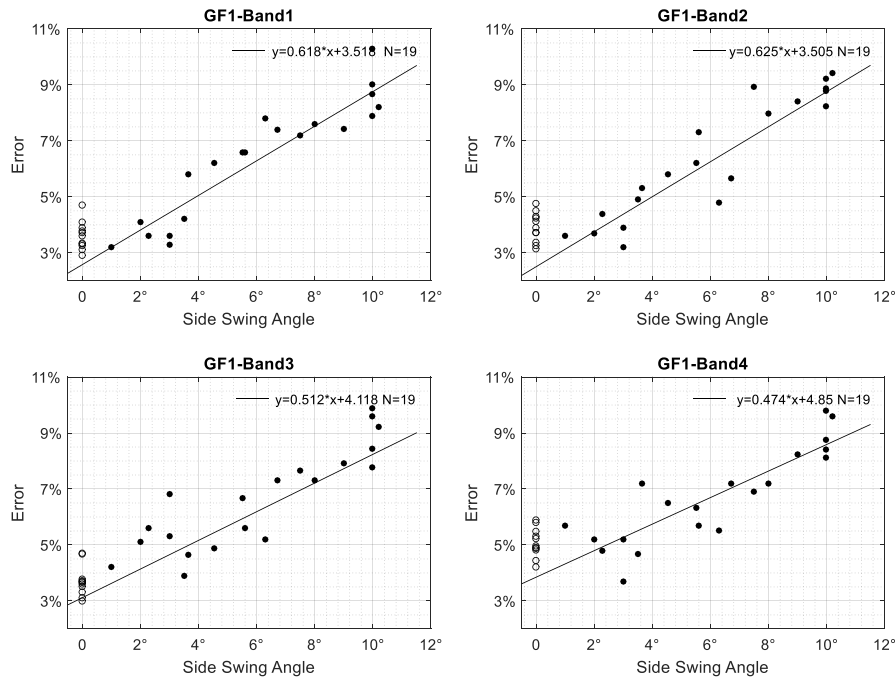
Figure 4: Side-swing angle and calibration error results for 2013-2018

4.3 Comparison of GF-1/WFV4 and MDOIS before and after calibration

The average error before and after calibration of the radiation cross-calibration is shown in Tab. 3. The average errors corresponding to the four bands of the GF-1/WFV4 camera are: 7.44%, 7.43%, 7.65% and 7.74%. The average errors are 2.38%, 2.45%, 1.81% and 1.37%. It can be seen from Tab. 3 that the average error of the four bands decreased by 5.56%, 4.98%, 5.84% and 6.37% after correction. The error of cross-calibration of the GF-1 and MODIS radiation is basically controlled within 5%, which improves the accuracy and frequency of radiometric calibration.

Table 3: Comparison of average errors before and after correction

Band	*Error-Before (%)*	*Error-After (%)*	*Error (%)*
Band1	7.44	2.38	5.06
Band2	7.43	2.45	4.98
Band3	7.65	1.81	5.84
Band4	7.74	1.37	6.37

5 Conclusion

This paper crosses the GF-1 wide coverage multi-spectral camera with reference to the band 1, 2, 3 and 4. Through the analysis of the research results, the radiation calibration can draw the following conclusions:

(1) Calculate the gain and error of each band of GF-1/WFV4 by cross-calibration linear regression method. The different images of the satellites are in accordance with the radiation cross-calibration conditions and the GF-1 satellites have no side swing angle. At this point, the radiation cross-calibration results have better radiation characteristics and the radiation accuracy is less than 5.5%. The calibration coefficients obtained by factors such as spectral response and observation time are stable and reliable.

(2) Through 19 sets of side swing angle's data and 10 sets of scenes without side swing angle, the radiation cross calibration is first performed to obtain their gain value and offset value, and then the single element linear fitting method is adopted. Obtain the relationship between the number of side swing angles and the error. Finally, the corresponding side swing angle is multiplied by the correction factor for each frequency band by linear correction, which greatly reduces the on-orbit radiation cross-calibration due to satellite side swing angles. This method further improves the accuracy of satellite radiation calibration.

References

Bai, Z. G. (2013): Technical characteristics of GF-1 satellite. *Aerospace China*, no. 8, pp. 5-9.

Duan, X. T.; Song, H. X.; Qin, C.; Muhammad, K. K. (2018): Coverless steganography for digital images based on a generative model. *Computers, Materials & Continua*, vol. 55, no. 3, pp. 483-493.

Gao, H. L.; Gu, X. F.; Yu, T.; Sun, Y.; Liu, Q. Y. (2016): Cross-calibration of GF-1 PMS sensor with Landsat 8 OLI and Terra MODIS. *IEEE Transactions on Geoscience & Remote Sensing*, vol. 54, no. 8, pp. 4847-4854.

Han, J.; Xie, Y. (2016)**:** Image dodging algorithm for GF-1 satellite WFV imagery. *Acta Geodaetica et Cartographica Sinica*, vol. 45, no. 12, pp. 1423-1433.

Liu, J.; Wang, L. M.; Yang, L. B.; Shao, J.; Teng, F. et al. (2015): Geometric correction of GF-1 satellite images based on block adjustment of rational polynomial model. *Transactions of the Chinese Society of Agricultural Engineering*, vol. 31, no. 22, pp. 146-154.

Lin, G. Y.; Liu, B. W.; Xiao, P. C.; Lei, M.; Bi, W. (2018): Phishing detection with

image retrieval based on improved texton correlation descriptor. *Computers, Materials & Continua*, vol. *57*, no. 3, pp. 533-547.

Qi, C.; Suzanne, M.; Sun, H. Y. (2018): Identifying materials of photographic images and photorealistic computer generated graphics based on deep CNNs. *Computers, Materials & Continua*, vol. 55, no. 2, pp. 229-241.

Wei, W.; Zhang Y. N.; Zhang, M.; Zhao, C. Y.; Li, X. et al. (2018): Multisite high-frequency radiometric calibration of GF-1 wide field of view. *Acta Photonica Sinica.*

Yao, Y.; He, J.; Zhang, J. B.; Zhang, Y. T. (2017): Extracting urban impervious surface from GF-1 imagery using one-class classifiers. arXiv:1705.04824.